Design and Numerical Characterization of a First Stage of a High Capacity Multistage Centrifugal Pump

Nicolas La Roche-Carrier, Guyh Dituba Ngoma and Walid Ghie
University of Quebec in Abitibi-Témiscamingue, School of Engineering's Department,
445, Boulevard de l'Université Rouyn-Noranda, Quebec, J9X 5E4, Canada

Keywords: Multistage Centrifugal Pump, Impeller, Diffuser, ANSYS-CFX, Modeling and Simulation.

Abstract: In this paper, a numerical characterization of a first stage of a high capacity multistage centrifugal pump was performed for very high flow rates. A particular emphasis was placed on the diffuser design procedure. For this purpose, the equations of the continuity and the Navier-Stokes accounting for the boundary conditions were used by mean of ANSYS-CFX code to describe and to simulate the complex liquid flow in the multistage centrifugal pump. In order to identify the key parameters of the diffuser that can improve the pump stage performances, the effects of the inlet height of the diffuser vanes, the number of the diffuser vanes, the number of the diffuser return vanes, and the gap between the impeller and the diffuser on the pump stage head, brake horsepower and efficiency were analyzed. The validation of the developed model of a first pump stage was done comparing results of numerical simulations and experimental results obtained from a pump manufacturer.

1 INTRODUCTION

Multistage centrifugal pumps are widely used in industrial and mining enterprises. They are composed of several stages. These last are constituted of an impeller, a diffuser and a casing. The diffuser is generally provided of the return vanes except the diffuser of the last pump stage. The impeller and the diffuser are the most important components of a multistage centrifugal pump. The performances of multistage pumps are depended to both components. The impeller must be designed to obtain a high head with an optimum efficiency, while the diffuser is designed to maximizer the pressure gain in the diffuser vanes and to minimize the pressure drop in the return vanes. Therefore, the relevant parameters of the impeller and the diffuser including the return vane must be determined with high precision in the planning, the design and the optimization phases in design and off-design conditions. This is to achieve better multistage centrifugal pump performances accounting for the three-dimensional and turbulent liquid flow in multistage centrifugal pumps. Many experimental and numerical studies have been conducted on multistage centrifugal pumps (Qihua Z. et al, 2013; La Roche-Carrier N. et al., 2013; Qihua Z. et al, 2012, and Miyano M. et al., 2008).Thorough analysis of previous works shows that there are several diffuser types. The design procedure of diffusers are not well detailed, while the design procedure for the impeller is well documented. The diffuser design depends on the experience of the designer and the information available. Moreover, analysis of previous studies clearly revealed that the research results obtained are specific to the design parameters and configuration of components in multistage centrifugal pumps, and thus cannot always be generalized. Therefore, in the present work, the goal is to enhance the design and the performances of multistage centrifugal pumps using rigorously the design procedure described in (Gülich, J. F., 2010) to model the diffuser including return vanes, as shown in Fig. 1. This diffuser must be allowed a higher pressure gain to the level of the diffuser vanes and a lower pressure lost in diffuser return vanes. To identify adequately diffuser parameters that could be enhance the performances of a first stage of a multistage centrifugal pump, a numerical investigation was conducted using ANSYS-CFX code (Ansys inc., 2015). This was done considering the three-dimensional turbulent liquid flow through a first stage of a multistage centrifugal pump account for various flow conditions and diffuser key

Roche-Carrier, N., Ngoma, G. and Ghie, W.
Design and Numerical Characterization of a First Stage of a High Capacity Multistage Centrifugal Pump.
DOI: 10.5220/0005995102830290
In *Proceedings of the 6th International Conference on Simulation and Modeling Methodologies, Technologies and Applications (SIMULTECH 2016)*, pages 283-290
ISBN: 978-989-758-199-1

parameters including the inlet height of the diffuser vanes, the number of the diffuser vanes, the number of the diffuser return vanes, and the gap between the impeller and the diffuser. Upon applying the equations of the continuity and the Navier-Stokes, the liquid flow velocity and the liquid pressure distributions in a stage of a multistage centrifugal pump were determined, while accounting for boundary conditions and considering a constant rotating speed for the impeller. The pump stage performances were represented as a function of the flow rate in each case study.

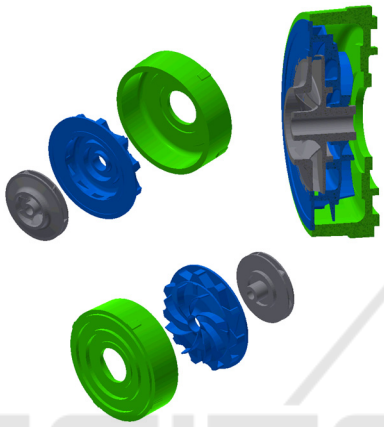

Figure 1: Modeled first stage of a multistage centrifugal pump.

2 GOVERNING EQUATIONS

The used fluid domains of the first stage obtained from Fig. 1 for the governing equations for liquid flow are shown in Fig. 2.

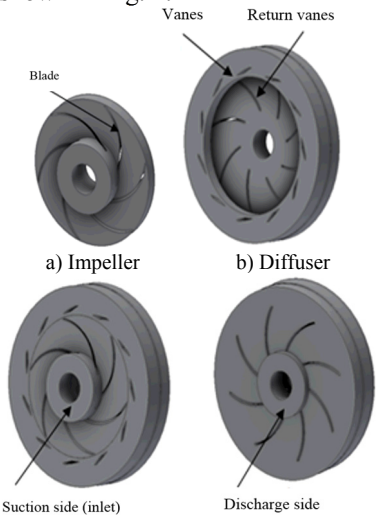

c) Stage: combined impeller and diffuser

Figure 2: Fluid domains of the first pump stage.

The following assumptions were made to describe the governing equations for liquid flow: (i) a steady state, three-dimensional and turbulence flow using the k-ε model was assumed; (ii) it was an incompressible liquid; (iii) it was a Newtonian liquid; and (iv) the liquid's thermophysical properties were constant with the temperature.

To account for these assumptions, the theoretical analysis of the liquid flow through the first pump stage was based on the equations of the continuity and the Navier-Stokes (Ansys inc., 2015). For the three-dimensional liquid flow through these components of a first pump stage as shown in Fig. 2, the equations of the continuity are expressed by:

$$\nabla.\vec{V}_{vel} = 0 \tag{1}$$

where $\vec{V}_{vel} = \vec{V}_{vel}(u(x,y,z), v(x,y,z), w(x,y,z))$ is the liquid flow velocity vector.

Using the coordinate system, Eq. 1 can be rewritten as:

$$\frac{\partial u}{\partial x} + \frac{\partial v}{\partial y} + \frac{\partial w}{\partial z} = 0 \tag{2}$$

and the equations of the Navier–Stokes are given by:

$$\begin{aligned} &\rho\nabla.(\vec{V}_{vel} \otimes \vec{V}_{vel}) = -\nabla p \\ &+ \mu_{eff}\nabla.(\nabla\vec{V}_{vel} + (\nabla\vec{V}_{vel})^T) + B \end{aligned} \tag{3}$$

where p is the pressure, ρ is the density, μ_{eff} is the effective viscosity accounting for turbulence, ⊗ is a tensor product and B is the source term. For flows in an impeller rotating at a constant speed ω, the source term can be written as follows:

$$B = -\rho\left(2\vec{\omega}x\vec{V}_{vel} + \vec{\omega}x\left(\vec{\omega}x\vec{r}\right)\right) \tag{4}$$

where $\vec{r}$ is the location vector, $2\vec{\omega}x\vec{V}_{vel}$ is the centripetal acceleration and $\vec{\omega}x\left(\vec{\omega}x\vec{r}\right)$ is the Coriolis acceleration.

B is zero for the flow in the stationary components like the diffuser. Using the coordinate system, Eq. 3 can be rewritten as:

$$\begin{aligned} &\rho\left(u\frac{\partial u}{\partial x} + v\frac{\partial u}{\partial y} + w\frac{\partial u}{\partial z}\right) = \mu_{eff}\left(\frac{\partial^2 u}{\partial x^2} + \frac{\partial^2 u}{\partial y^2} + \frac{\partial^2 u}{\partial z^2}\right) \\ &-\frac{\partial p}{\partial x} + B_x \\ &\rho\left(u\frac{\partial v}{\partial x} + v\frac{\partial v}{\partial y} + w\frac{\partial v}{\partial z}\right) = \mu_{eff}\left(\frac{\partial^2 v}{\partial x^2} + \frac{\partial^2 v}{\partial y^2} + \frac{\partial^2 v}{\partial z^2}\right) \\ &-\frac{\partial p}{\partial y} + B_y \\ &\rho\left(u\frac{\partial w}{\partial x} + v\frac{\partial w}{\partial y} + w\frac{\partial w}{\partial z}\right) = \mu_{eff}\left(\frac{\partial^2 w}{\partial x^2} + \frac{\partial^2 w}{\partial y^2} + \frac{\partial^2 w}{\partial z^2}\right) \\ &-\frac{\partial p}{\partial z} + B_z \end{aligned} \tag{5}$$

where

$$B_x = \rho(\omega_z^2 r_x + 2\omega_z v)$$
$$B_y = \rho(\omega_z^2 r_y - 2\omega_z u) \quad (6)$$
$$B_z = 0$$

Furthermore, μ_{eff} is defined as $\mu_{eff} = \mu + \mu_t$, where μ is the dynamic viscosity and μ_t is the turbulence viscosity.

Since the k-ε turbulence model is used in this work because convergence is better than with other turbulence models, μ_t is linked to turbulence kinetic energy k and dissipation ε.

To solve equations 2 and 5 numerically while accounting for the boundary conditions and turbulence model k-ε, the computational fluid dynamics ANSYS-CFX code, based on the finite volume method, was used to obtain the liquid flow velocity and pressure distributions. According to the boundary conditions, they were formulated as follows: the static pressure provided was given at the stage inlet, while the flow rate provided was specified at the stage outlet. The frozen rotor condition was used for the impeller-diffuser interface. A no-slip condition was set for the flow at the wall boundaries.

The performance parameters of the first pump stage are described as follows:

The pump stage head is given by $H = (p_{to} - p_{ti}) / \rho g$,

where p_{ti} is the total pressure at the pump stage inlet and p_{to} the total pressure at the pump stage outlet.

Furthermore, the hydraulic power of the pump stage is formulated as $P_h = \rho Q g H$, where Q is the flow rate.

In addition, the brake horsepower of the pump stage is given by $P_s = T\omega$, T is the impeller torque.

From the hydraulic power and the brake horsepower, the efficiency of the pump stage can be written as

$$\eta = P_h / P_s.$$

3 DESIGN PROCEDURE OF THE DIFFUSER

The diffuser including the return vanes were designed in this work according to the book of Gülich (Gülich, J. F., 2010) with respect of the design conditions for first pump stage such as the head, the flow rate and the rotating speed. Fig. 3 shows the geometrical main parameters of the considered diffuser.

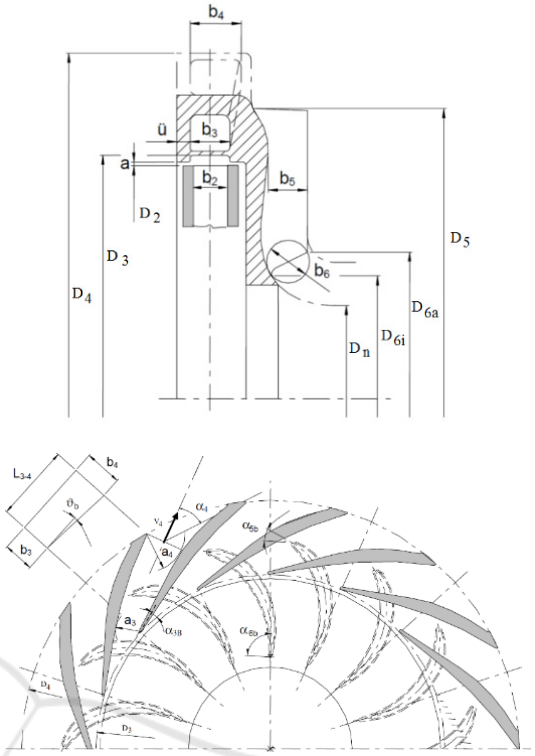

Figure 3: Design parameters of a diffuser including of return vanes (Gülich, J. F., 2010).

3.1 Design of the Diffuser Vanes

The inlet height of the diffuser vanes b_3 is calculated using the following equation:

$$b_3 = (1.05 \text{ to } 1.3) \cdot b_2 \quad (7)$$

where b_2 is the impeller outlet height.

The inlet angle of the diffuser vane α_{3b} can be defined by:

$$\alpha_{3b} = \alpha_3 \pm 3^\circ \quad (8)$$

where $\alpha_3 = \tan^{-1}\left(\frac{V_{m3}}{V_{u3}}\right)$, V_{u3} is the tangential component of absolute velocity of diffuser inlet, and V_{m3} is the meridional component of absolute velocity at diffuser inlet.

V_{m3} is given by:

$$V_{m3} = \frac{Q \cdot \tau_3}{\pi \cdot D_3 \cdot b_3} \quad (9)$$

where τ_3 is the blade blockage factor (supposed to be 1) and D_3 is the diffuser inlet diameter

Additionally, V_{u3} can be expressed as:

$$V_{u3} = V_{u2} \cdot \left(\frac{D_2}{D_3}\right) \quad (10)$$

where V_{u2} is the tangential component of absolute velocity at impeller outlet. It is given by:

$$V_{u2} = \frac{gH}{\eta_h U_2} + \frac{U_{1m} V_{1u}}{U_2} \quad (11)$$

Moreover, the vane number of the diffuser Z_{Le} is chosen as a function of the blade number of the impeller Z_b according to Tab. 1.

Table 1: Number of blades required for the diffuser (Gülich, J. F., 2010).

Z_b	5			6	7				
Z_{Le}	7	8	12	10	9	10	11	12	(15)

Furthermore, the diffuser inlet wide is formulated as

$$a_3 = f_{a3} \cdot \left(\frac{D_3}{2}\right) \cdot \left\{ \exp\left(\frac{Q}{b_3 \cdot V_{2u} \cdot \left(\frac{D_2}{2}\right) \cdot Z_{Le}} \right) - 1 \right\} \quad (12)$$

where f_{a3} is the correction factor. Its value is between 1.1 and 1.3.
The diffuser vane inlet thickness can be expressed as:

$$e_3 = (0.01 \text{ à } 0.015) \cdot D_2 \quad (13)$$

Additionally, the diffuser outlet diameter is given by:

$$D_4 = ((1.05 \text{ à } 1.15) + 0.01 \cdot n_q) \cdot D_2 \quad (14)$$

where n_q is the specific speed.

The diffuser opening angle ϑ_b is expressed as:

$$\vartheta_b = \tan^{-1}\left(\frac{0.5 \cdot (a_4 - a_3)}{L_{3-4}} \right) \quad (15)$$

where L_{3-4} is the length of the vane passage of diffuser and a_4 is the diffuser outlet wide.

Furthermore, the outlet height of the diffuser vane is given by:

$$b_4 = b_3 + (\tan(\vartheta_b) \cdot L_{3-4}) \quad (16)$$

3.2 Design of the Diffuser Return Vanes

The number of return vanes Z_R is chosen with respect to the relationship $Z_R \leq Z_{Le}$ in order to allow the liquid flow to defect sufficiently in the return vane passages. The thickness of the diffuser return vanes e_6 is estimated based on the experience of the designer. Moreover, the inlet height of the diffuser return vanes b_5 is supposed to be equal to the outlet height of the diffuser return vanes b_6. It can be formulated as follows:

$$b_5 = b_6 = \frac{Q}{\pi \cdot D_6 \cdot V_{m6}} \quad (17)$$

where D_6 is the diameter at the diffuser return vane outlet, by hypothesis, it is equal to the diameter at the inlet of the impeller D_1, and V_{m6} is the meridional velocity at the return vanes outlet. It is given by:

$$V_{m6} = (0.85 \text{ à } 0.9) \cdot V_{m1} \quad (18)$$

Furthermore, the flow angle at the diffuser return vane inlet is expressed as:

$$\alpha_5 = \tan^{-1}\left(\frac{V_{m5}}{V_{u5}} \right) \quad (19)$$

Where

$$V_{m5} = \frac{Q}{\pi \cdot D_5 \cdot b_5} \quad (20)$$

$$V_{u5} = V_{u4} \cdot \left(\frac{D_4}{D_5}\right) \quad (21)$$

$$V_{u4} = V_{u3} \cdot \left(\frac{D_3}{D_4}\right) \quad (22)$$

In addition, the flow angle at the outlet of the return vanes α_{6b} is formulated as:

$$\alpha_{6b} = \alpha_6 \pm 5° \quad (23)$$

where the outflow angle is supposed to be $\alpha_6 = 90°$.

4 RESULTS AND DISCUSSION

The working liquid water was used for all simulation runs in this study. It was considered to have the following reference values at 25 °C: dynamic viscosity of 8.899 x 10^{-4} Pas and density of 997 kg/m³. The main reference data for the impeller, the diffuser and diffuser return vanes are given in Tabs. 1-3 respectively.

To identify the parameters of the first stage of a multistage centrifugal pump that were influenced their performances, five key parameters were selected taking account to the diffuser including the return vanes: a) diffuser inlet height (31,75 mm; 41,98 mm; 50,8 mm), b) number of diffuser Vanes (9, 10,11), c) number of diffuser return vanes (7, 8, 9), and d) gap between the impeller and the diffuser (75%; 81.25%; 87.5%; 93.75%; 100% of the impeller outlet diameter).

Table 2: Impeller.

Inner diameter [mm]	195
Outer diameter [mm]	406
Number of blades	6
Blade inlet angle [Degree]	18
Blade outlet angle [Degree]	22.5
Blade thickness [mm]	7.94
Blade inlet height [mm]	56
Blade outlet height [mm]	41.98
Number of blades	6
Hub diameter	84.84
Rotating speed [rpm]	1750

Table 3: Diffuser.

Inner diameter [mm]	407.016
Outer diameter [mm]	572.42
Number of vanes	11
Vane inlet angle [Degree]	10
Inlet height of flow passage [mm]	41.98
Outlet height of flow passage [mm]	75.39
Inlet width of flow passage [mm]	18.71
Vane thickness [mm]	6

Table 4: Diffuser return vanes.

Inner diameter [mm]	459
Outer diameter [mm]	194.95
Number of return vanes	8
Inlet angle [Degree]	21
Outlet angle [Degree]	95
Outlet height of flow passage [mm]	14.14
Thickness [mm]	6.35

Mesh-independent solution tests have been carried out with highest accuracy using different numbers of mesh elements in each case study.

4.1 Effect of the Inlet Height of Diffuser Vanes

To investigate the effect that the inlet height of the diffuser vanes has on the pump stage performances, the vane inlet height of 31.75 mm, 41.98 mm and 50.8 mm were selected supposing that the outlet height of the impeller blade was equal to the inlet height of the diffuser vane, while other parameters were keep constant. Fig. 4 shows the pump head as a function of the flow rate with the inlet height of the diffuser vanes as parameter. From this figure, it is to assess that the pump head increases with increasing inlet height of the diffuser vanes. By fixed the flow rate, this can be explained by the fact that the meridional velocity at the outlet of the impeller decreases with increasing outlet height of the impeller blades that is equal to the inlet height of the diffuser vanes. The liquid pressure drops in the impeller, and the diffuser decreases with increasing inlet height of the diffuser vanes. This leads to the increase of the static pressure in the first pump stage. Moreover, Tab. 5 indicates the pressure difference for 700 m³/h in the impeller, the diffuser, and the diffuser return vane passages. There, it can be observed that the pressure gain in diffuser increases with increasing inlet height of the diffuser, and the pressure loss in the diffuser return vane passages decreases, while the impeller head rises. The total pressure difference is highest for a diffuser inlet vane height of the 50.8 mm.

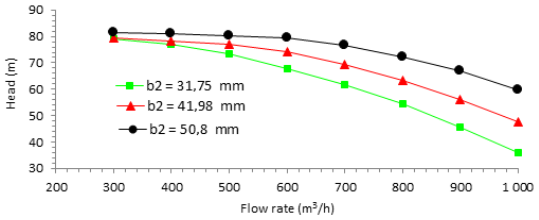

Figure 4: Pump stage head versus flow rate.

Table 5: Distribution of pressure difference for 700 m³/h.

Inlet height of the diffuser vane [mm]	Pressure difference Δp [Pa]			
	Impeller	Diffuser	Diffuser return vane passages	Δp_{total}
31.75	574 849	98 063	-71 039	601 874
41.98	631 536	119 480	-74 264	676 752
50.80	682 690	136 546	-70 367	748 869

Moreover, the corresponding curves of the pump stage brake horsepower as a function of the flow rate are shown in Fig. 5, illustrating that the brake horsepower increases with increasing inlet height of the diffuser vanes. This can be explained by the fact that the brake horsepower increases relative to the outlet height of the impeller blade and the inlet height of the diffuser vane due to the requested increase in pump shaft torque relative to the increased diffuser vane height and impeller blade height.

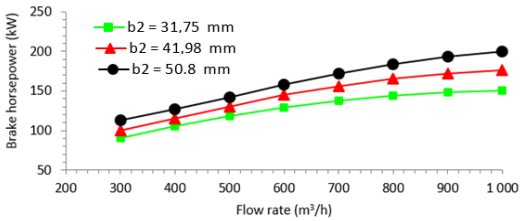

Figure 5: Brake horsepower versus flow rate.

Furthermore, the curves representing pump stage efficiency as a function of the flow rate is represented in Fig. 6, where it is observed that the efficiency for the inlet height of the diffuser vane of 50.8 mm is the lowest for the flow rate below of 700 m³/h, while it is the highest for the flow rate above 700 m³/h.

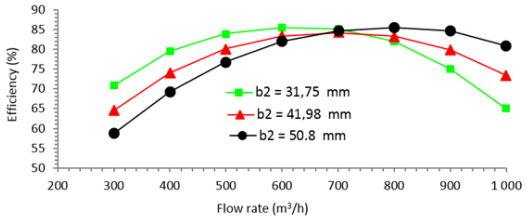

Figure 6: Pump stage efficiency versus flow rate.

4.2 Effect of the Number of the Diffuser Vanes

Three diffuser vanes numbers (9, 10 and 11) were selected to analyze it effect on the pump stage head, brake horsepower, and efficiency, while other parameters were kept constant. Fig. 7 shows the head as a function of the flow rate. There, it can be seen that the head is only slightly affected by the number of the diffuser vanes.

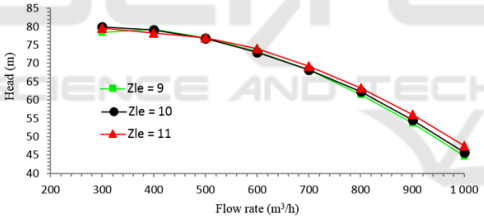

Figure 7: Pump stage head versus flow rate.

Additionally, the corresponding curves of the brake horse power as a function of the flow rate is shown in Fig. 8, there it can be seen the variation in the number of the diffuser vanes don't nearly affect the brake horsepower.

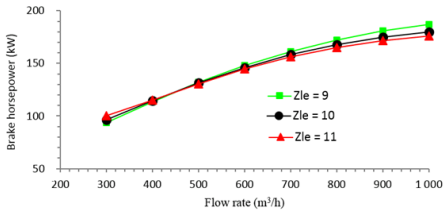

Figure 8: Brake horsepower versus flow rate.

Furthermore, Fig. 9 represents the efficiency as a function of the flow rate. From this figure, it is observed that the highest efficiency was obtained for the diffuser vane number of 11 for a flow rate higher than 480 m³/h.

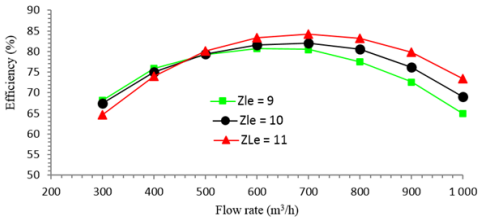

Figure 9: Pump stage efficiency versus flow rate.

Moreover, Tab. 6 indicates the distribution of the pressure difference in the impeller, the diffuser, and the diffuser return vane passages for a flow rate of 700 m³/h. From this table, it is observed that the increase of the diffuser vane number leads to the decrease of the impeller head, while the pressure gain in the diffuser rises and the pressure loss in the diffuser return vane passages decreases. But, globally, the head of the pump stage is not nearly influenced by the variation of the diffuser vane number.

Table 6: Distribution of pressure difference for 700 m³/h.

	Pressure difference Δp [Pa]			
Diffuser vane number	Impeller	Diffuser	Diffuser return vane passages	Δp_{total}
9	649 275	97 114	-78 487	667 902
10	636 433	108 425	-76 866	667 991
11	631 536	119 480	-74 264	676 752

4.3 Effect of the Number of Diffuser Return Vanes

To examine the effect of the number of diffuser return vanes on the performances of the pump stage, three diffuser models with 7, 8 and 9 return vanes were selected, while other parameters were kept constant. Figs. 10-12 show that the variation in the number of diffuser return vanes don't nearly influence the head, brake horsepower and the efficiency of pump stage, in spite of a light increase of the head and the efficiency of the diffuser with 9 return vanes.

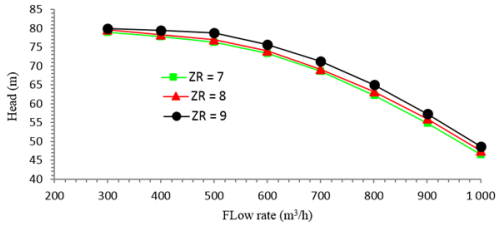

Figure 10: Pump stage head versus flow rate.

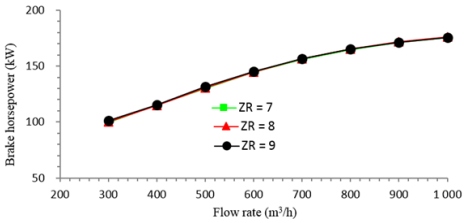

Figure 11: Brake horsepower versus flow rate.

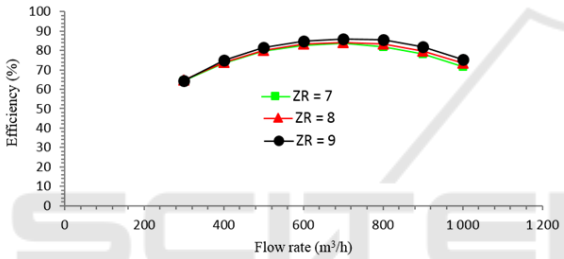

Figure 12: Pump stage efficiency versus flow rate.

4.4 Effect of Gap between the Impeller and the Diffuser

To investigate the effect of the gap between the impeller and the diffuser on the performances of the pump stage, the impeller outer diameter values of 406.4 mm (impeller diameter ratio: 100 %), 381mm (impeller diameter ratio: 93.75 %), 355.6 mm (impeller diameter ratio: 87.5 %), 330.2 mm (impeller diameter ratio: 81.25 %) and 304.8 mm (impeller diameter ratio: 75 %) were selected when keeping other parameters constant. Fig. 13 shows the head of the pump stage as a function of the impeller diameter ratio for the flows rates of 500 m^3/h, 700 m^3/h and 900 m^3/h. From this figure, it can be seen that the pump stage head increases with decreasing gap between the impeller and the diffuser. This can be explained by the fact that the pressure difference between the impeller outlet and inlet decreases with increasing impeller diameter ratio maintaining the diffuser inner diameter constant.

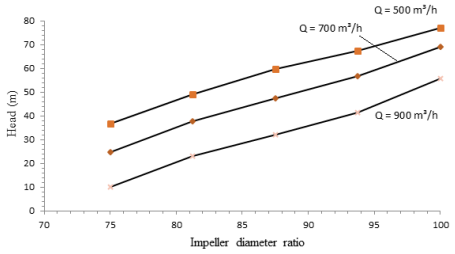

Figure 13: Pump head versus flow rate.

Furthermore, Fig. 14 shows that the brake horsepower increases with decreasing gap between the impeller and the diffuser due to the requested augmented impeller shaft torque relative to the size of the impeller diameter keeping the diffuser inner diameter constant. Additionally, the corresponding efficiency curves as a function of the flow rate presented in Fig. 15 indicate that the level of the flow rate and the impeller diameter ration have an impact on achieving a better efficient.

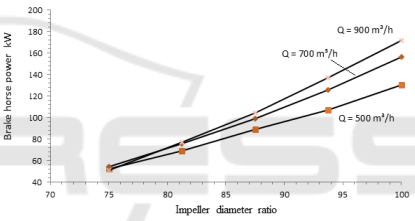

Figure 14: Brake horsepower versus flow rate.

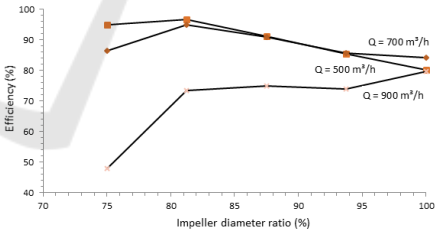

Figure 15: Efficiency versus impeller diameter ratio.

4.5 Model Comparison

The developed model of a first stage of a multistage centrifugal pump using the design procedure described in (Gülich, J. F., 2010) was validated comparing the numerical simulation results with the experimental results obtained from a pump manufacturier (Technosub Inc.). Fig. 16 show that the numerical curves are in good agreement with the experimental curves.

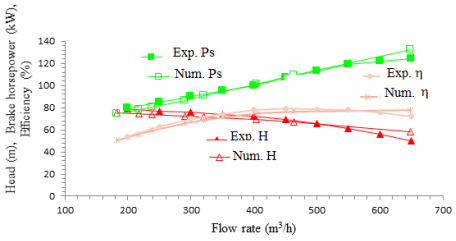

Figure 16: Results comparison.

5 CONCLUSION

In this study, the design procedure described in "Gülich, J. F., 2010" for the diffuser including the return vanes was used to model a diffuser in order to identify the diffuser parameters that improve the pump stage performances. To this effect, a complex liquid flow model in a pump stage was developed to analyze the effects of the inlet height of the diffuser vanes, the number of the diffuser vanes, the number of the diffuser return vanes, and the gap between the impeller and the diffuser on the pump stage head, brake horsepower and efficiency. The achieved results for considered value ranges reveal, among others, that the diffuser height strongly influences the pump stage performances. The variations in the number of the diffuser vanes and of the diffuser return vanes slightly affect the pump stage performances. Moreover, the gap between the impeller and the diffuser affects the pump stage performances dependently of the impeller diameter ratio. The comparison of numerical simulation results from the developed model with experimental results obtained from a pump manufacturer shows good harmony.

ACKNOWLEDGMENTS

The authors are grateful to the company Technosub inc. (pump manufacturer) in Rouyn-Noranda, Quebec, Canada.

REFERENCES

Gülich, J. F., 2010. *Centrifugal Pumps*, second Edition, Springer.

Qihua Z., Weidong S., Yan X., Xiongfa G., Chuan W., Weigang L., and Dongqi M. 2013. A New Proposed Return Guide Vane for Compact Multistage Centrifugal Pumps. *International Journal of Rotating Machinery,* Volume 2013, Article ID 683713, 11 pages.

La Roche-Carrier N., Dituba Ngoma G., and Ghie W., 2013. Numerical investigation of a first stage of a multistage centrifugal pump: impeller, diffuser with return vanes, and casing. *ISRN Mechanical Engineering*, Volume 2013, Article ID 578072, 15 pages.

Qihua Z., Yan X., Weidong S., Weigang L., Ling Z. 2012. Research and development on the Hydraulic Design System of The Guide Vanes of Multistage Centrifugal Pumps. *Applied Mechanics and Materials*.

Miyano M., Kanemoto T., Kawashima D., Wada A., Hara T., Sakoda K., 2008. Return Vane Installed in Multistage Centrifugal Pump. *International Journal of Fluid Machinery and Systems*, Vol. 1, No. 1.

Ansys inc. 2015. *ANSYS-CFX (CFX Introduction, CFX Reference Guide, CFX Tutorials, CFX-Pre User's Guide, CFX-Solver Manager User's Guide, CFX-Solver Modeling Guide, CFX-Solver Theory Guide)*, release 16.2, USA.

Technosub Inc., www.technosub.net.